Journal of the Brazilian Society of Mechanical Sciences and Engineering (2024) 46:369
https://doi.org/10.1007/s40430-024-04944-5

TECHNICAL PAPER

ANN model of a triple-junction cell in concentrating photovoltaic system

C. Renno[1] · A. Perone[1] · O. Di Marino[1]

Received: 12 January 2024 / Accepted: 22 April 2024

Abstract

Significant advancements in concentrating photovoltaic (CPV) systems have been achieved in recent years, also thanks to the definition of calculation methods of their energy performances in several operation conditions. Typically, the CPV systems electrical power is separately calculated or in terms of its temperature or concentration factor (C), but not simultaneously in terms of both variables. In this paper, an Artificial Neural Network model based on experimental data, linking electric power of CPV system with Direct Normal Irradiance and Triple-Junction cell temperature for different C values, is developed. Moreover, the model is also adopted to realize a feasibility analysis of point-focus CPV system used for different users: residential building and agricultural livestock farm. The optimal number of modules is determined to maximize the Net Present Value (NPV) of the investment. For the residential user, an optimal configuration of CPV system includes 16 modules, providing a peak power of 3.1 kW and covering an area of 130 m^2. This configuration allows the maximization of NPV value, reaching 15.9 k€, with DPB of 9.8 years. As for the agricultural livestock, 36 modules, with peak power of 7.0 kW and covering an area of 292 m^2, allow the maximization of NPV value equal to 16.3 k€, with DPB of 10.2 years.

Keywords CPV/T system · Point-focus configuration · Triple-Junction cell · ANN model · Experimental analysis

Abbreviations

C	Concentration factor
CPV	Concentrating photovoltaic system
CPV/T	Concentrating photovoltaic and thermal system
DNI	Direct normal irradiance (kW/m^2)
f	Non-ideal tracking system factor
I	Concentrated solar radiation (kW/m^2)
n	Number
P	Electric power (W)
E	Electric energy (Wh)
p_{par}	Parasitic current losses
T	Temperature (°C)
TJ	Triple-junction cell
η	Electrical efficiency
NPV	Net present value (€)
DPB	Discounted payback period (years)

Subscripts

el	Electrical
env	Environmental
exp	Experimental
inv	Inverter
mod	Module
opt	Optical
th	Theoretical

1 Introduction

Due to increasing environmental pollution, renewable technologies [1] are playing a crucial role referring to energy production [2] to match the energy requirements of different users [3]. Solar energy represents a resource widely available and is the most promising in terms of sustainability and development potential among all renewable energy sources [4]. In last years, the concentrating photovoltaic (CPV) systems have been subjected to a fast development [5]. In CPV system, the Direct Normal Irradiance (DNI) is concentrated by optics of large area on Multi-Junction (MJ) cells with high efficiency [6]. In this way, higher efficiency can be achieved for surface area unit than conventional photovoltaic systems (PV), in

Technical Editor: Ahmad Arabkoohsar.

✉ C. Renno
crenno@unisa.it

[1] Department of Industrial Engineering, University of Salerno, Via Giovanni Paolo II, 132, 84084 Fisciano, SA, Italy

Published online: 20 May 2024

proportion to the concentration factor, adopting cheap mirrors or lenses [7, 8]. In order to reduce system costs, MJ cells are adopted under high irradiance, and consequently, in conditions of high temperatures resulting in decrease of the photoelectric conversion efficiency of solar cells. High cell temperatures not only lead to reduction of efficiency but can also cause permanent damage to cell. Therefore, it becomes essential to adopt a cooling system to maintain the cells in optimal working conditions.

Thermal energy can be recovered by MJ cells through an active cooling system [9]. Hence, the global efficiency of the concentrating photovoltaic and thermal (CPV/T) systems can be increased when electrical and thermal energies are simultaneously produced [10]. The CPV systems are more complex if compared to traditional PV systems [10] and it is not possible to have a standard configuration [11]. Several CPV systems different for optical, photovoltaic and thermal characteristics, are present in literature [12]. In fact, CPV systems are currently in developmental stage, with new designs and materials still being created to reduce energy cost [12]. Hence, the definition of methods for the calculation of their energy performances in different operation conditions constitutes an important step in this development process.

In literature, several models allow to evaluate electric power and temperature of TJ cell, parameters necessary to determine the CPV/T system performances from the electrical and thermal point of view. Among the different typologies of modeling, the Artificial Neural Networks (ANN) constitutes an interesting instrument for the energy performances evaluation [13]. For example, in [14], a method based on ANN which links current–voltage curves of HCPV module with atmospheric parameters, is studied. In [15], ANNs are adopted to forecast the CPV module maximum power using as input: air temperature, direct irradiance, solar spectrum and wind speed. In [16], an ANN with variable step size is used to determine the maximum power point tracking (MPPT) in photovoltaic plants. ANN models are also used for forecasting the solar radiation [17], which significantly influences the CPV systems energy outputs. Therefore, it is clear that models adopting ANNs represent a good solution when many physical variables influence the phenomena.

In particular, in this paper an ANN model based on experimental data is studied. The model links directly the electric power generated by CPV system with DNI and TJ cell temperature for a wide range of C values. Generally, the electrical power of CPV system is evaluated separately according to its temperature or solar concentration factor, but not simultaneously in terms of both variables. This innovative aspect is fundamental to evaluate the real performances of a CPV system when it has to be sized [18], adopting a modular configuration, to meet the energy demands of user.

Finally, the model has been used to analyze the monthly electrical producibility of CPV system applied to two different users, a residential building and a livestock farm located in Salerno (Italy). Moreover, for each user, the optimal number of modules has been defined to maximize the investment profitability evaluated in terms of Net Present Value (NPV).

2 Experimental setup

The CPV system, built in Applied Thermodynamics Laboratory of University of Salerno, is showed in Fig. 1 [19]. The CPV system consists mainly of receiver, optics and tracking system. Primary optics presents a point-focus configuration where a Fresnel lens of acrylic material, of 30 cm in diameter and 0.4 cm in thickness, is adopted. The receiver consists of Triple-Junction (TJ) cell positioned at lens focus and a passive cooling system. TJ solar cell is composed of InGaP/GaAs/Ge and presents an area of 5.5×5.5 mm^2 (Table 1). A kaleidoscope works as secondary optics to make homogeneous the incident radiation for unit of cell area, mitigating the chromatic aberration and increasing the optical efficiency. Because the CPV system works only with direct solar component, a tracking system is used in experimental plant to maximize the DNI on receiver.

The experimental plant has some degrees of freedom, permitting both solar tracking and concentration factor (C) variation; three degrees of freedom are available. The first two allow solar tracking through rotation both in horizontal plane to follow the sun in azimuth direction and in vertical

Fig. 1 Photo of the experimental CPV system

Table 1 Parameters of the Triple-Junction cell

Parameter	Value
Material	InGaP/InGaAs/Ge
Dimensions	5.5×5.5 mm
η_r(at 25 °C, 50 W/cm^2−1000 suns)	39.0%
Temperature coefficient (σ_t)	−0.04%/K
V_{oc}(at 25 °C, 50 W/cm^2−1000 suns)	2.94 V
I_{sc}(at 25 °C, 50 W/cm^2−1000 suns)	4.49 A

plane to track the sun in zenithal direction. Additionally, the TJ solar cells can be positioned at variable distance from primary optics, considering the focal length as additional freedom degree in experimental tests. In particular, the experimental system allows to move the Fresnel lens, located perpendicularly to sunrays, on vertical axis to adjust its height respect to TJ cell; hence, incident solar radiation can be varied on TJ cell changing C.

Figure 2 illustrates the measurement sensors adopted in the experimental plant. PT100 thermo-resistances, with accuracy of ± 0.2 °C, measure cell and outdoor temperatures; pyrheliometer, with accuracy of 2%, measures DNI. The TJ cell is linked to variable load, and an acquisition data system records experimental measurements of voltage, current, DNI and temperature. Moreover, the C direct measurement has been realized with an experimental procedure. The optical concentration factor (C_{opt}) is calculated as ratio between solar radiation concentrated on solar cell (I_{cell}) and DNI, representing the incident power flow on optical system:

$$C_{opt} = \frac{I_{cell}}{DNI} \quad (1)$$

Hence, C_{opt} is independent of TJ cell electrical performances, depending only on system optical performances. The measurement of I_{cell} was conducted using a thermal power sensor (accuracy ± 3%). It presents a series of bimetallic junctions (thermopile). The heat flow through the sensor generates voltage proportional to absorbed power when it flows through the thermopile. To ensure the comparability of measurements obtained by thermal power sensor and pyrheliometer, a precise calibration of thermal power sensor was carried out. In particular, it is necessary that solar radiation concentrated on TJ cell and power sensor are the same during the C_{opt} measurement. Finally, both TJ cell and power sensor were installed in parallel with same kaleidoscope to achieve an equal power flux, as illustrated in the Figs. 1 and 2.

3 ANN model

The main aim of paper is the study of an ANN model that links electric power generated by CPV system with solar radiation and TJ cell temperature when C_{opt} varies. The modeling adopts experimental data collected during the CPVsystem working. The first step of such study has been the identification of main model variables. Several variables affect the operation of CPV system and its energy performances. They can be divided in: external input

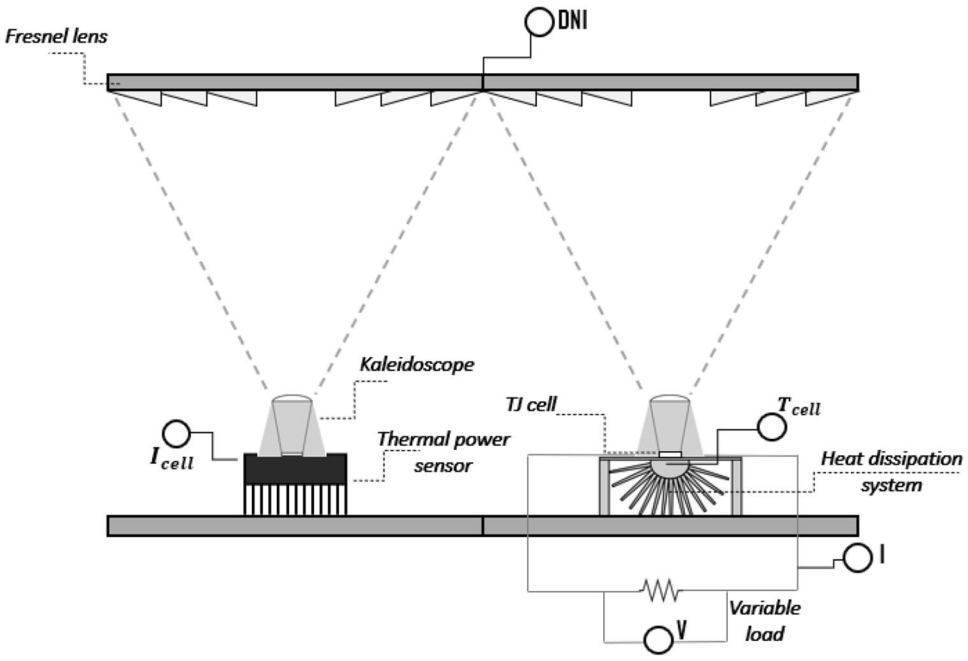

Fig. 2 Scheme of the measurement sensors

variables (Direct Normal Irradiance (DNI), environment temperature (T_{env})); internal variables (optical concentration factor (C_{opt}), TJ cell electrical efficiency (η_{cell})); output variables (TJ cell temperature (T_{cell}) and electric power supplied by TJ cell ($P_{el,cell}$) obtained by photo-generated current ($I_{ph,cell}$) and voltage (V_{cell})). The development of an ANN model requires many data, measured through the point-focus CPV system realized at Applied Thermodynamics Laboratory of University of Salerno and previously described. The experimental tests were conducted between January and July 2023 in different weather conditions and with sampling interval of 15 s. The experimental range of the monitored variables is shown in Table 2. Specifically, the variables DNI and C_{opt} have been combined with single parameter $I_{cell} = DNI \cdot C_{opt}$.

In order to evaluate the CPV system performances, the input data necessary for the ANN model are I_{cell} and T_{cell}, while the model output is the electric power supplied by TJ cell ($P_{el,cell}$). An ANN is mathematical tool employed for many purposes: classification, data mining, pattern recognition, image compression, process modeling, etc. [20]. Its functioning is inspired by human nervous system [21], comprising interconnected and layered neurons (nodes or units) with weighted connections. These weights are calculated by training algorithm, and each neuron computes a weighted sum based on input variables values. As the number of available data increases, ANN neural networks learn and return optimal results. The output of each neuron is determined by a transfer function as weighted sums of input [22].

An ANN can be treated as black-box model, because relationships between input and output are not necessary. ANN modeling needs to define typology of network, topology, training paradigm and transfer function. The most used type of connection for the data transfer is the multi-layer perceptron (MLP). A MLP operates as a feed-forward ANN, enabling the transmission of data from the input layer to the output layer through different number of hidden layers, all without including feedback loop. The hidden layers represent the ANN core. MLP networks have the capability to learn complex relationships between input and output, with good approximation. They generally use the error back-propagation (BP) algorithm as learning rule where the weights are updated according to the error function [22]. The best ANN topology can be definited through cross-validation, a validation technique able to estimate how a model generalizes an independent data set. The k-fold cross-validation technique is used to evaluate the mean squared error (MSE) defining the fitting assessment. The MSE outputs can be adopted to identify the optimal set of ANN parameters and to choose the best model between different plausible ANN alternatives [23]. As for training algorithm, BP paradigm allows the comparison between gradient descent with the momentum and weight decay to Levenberg–Marquardt algorithm [24]. Subsequently, ANN topology, number of hidden layers and neurons and transfer functions must be specified. Once set the ANN structure, three steps are necessary: learning, validation and test. The initial two steps involve network training and neurons parameter configuring, such as weights and bias. The third step incorporates new data in order to assess the network prediction capability through error analysis [25].

In particular, in this paper two different ANN models linking $P_{el,cell}$ to I_{cell} and T_{cell} have been developed in Matlab [26], valid in two ranges:

$$15\text{kW/m}^2 < I_{cell} < 70\text{kW/m}^2 \text{ and } 15°\text{C} < T_{cell} < 50°\text{C} \quad (2)$$

$$70\text{ kW/m}^2 < I_{cell} < 290\text{kW/m}^2 \text{ and } 22°\text{C} < T_{cell} < 70°\text{C} \quad (3)$$

Case 1 takes into account low C_{opt} values and Case 2 middle-high C_{opt} values. For both ANN models, the selected network is MLP with two input neurons (corresponding to I_{cell} and T_{cell}) and hidden layer with ten neurons (Fig. 3). Each network employs log-sigmoid function from input to hidden layer and tan-sigmoid function from hidden to output layer [22]. Many dataset for training, validation, and testing are necessary for the ANNs planning. They was obtained by measurements conducted adopting a point-focus CPV system realized at Applied Thermodynamics Laboratory of University of Salerno. The data pre-process is essential to obtain an ANN training as efficient as possible. Initially, abnormal data were excluded and then normalization was applied to mitigate the influence of variables measurement units and the range magnitude during training. Using the Matlab function ‘‘mapminmax”, a normalization interval [− 1, 1] was defined.

The data have been separated in three sets: training (70%), validation (15%) and test (15%). The first set is adopted in training phase to estimate the gradient and to update the network weights and biases through the training algorithm. The validation set is used to calculate the error, preventing overfitting. If the network data present overfitting, the validation error generally increases after an initial decrease. To enhance the network generalization capability, the early stopping technique is adopted. This technique saves network

Table 2 Monitored variables and their variation ranges

Monitored variable	Variation range
DNI	$300 \div 930\text{W/m}^2$
C_{opt}	$50 \div 310$
T_{env}	$12 \div 33°\text{C}$
I_{cell}	$15.0 \div 290\text{kW/m}^2$

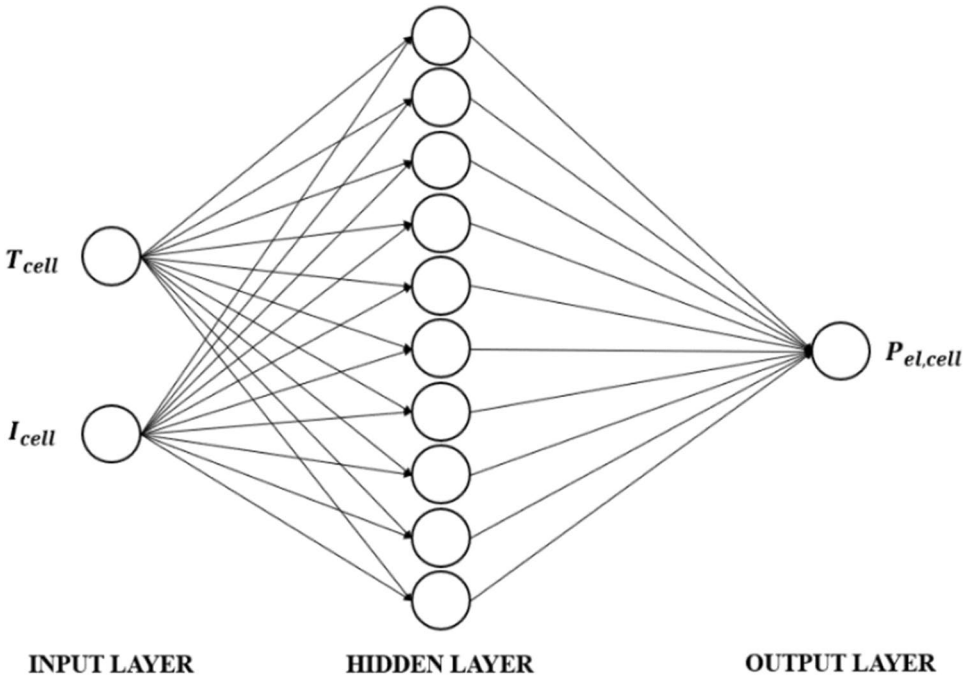

Fig. 3 Structure of the proposed neural networks in the two cases

weights and biases when the minimum validation error is reached. The third data set is used during test phase to confirm the network predictive power and to compare several models. When the test phase is finished, the ''mapminmax" function is also adopted in post-processing to return the outputs to the original domain.

The scatterplots of measured and predicted values for the three phases of training, validation and test for the cases 1 and 2 are reported in Figs. 4 and 5. The scatterplots provide significant information about the correlation between measured and predicted data. Figures 4 and 5 show in each of the three phases output points close to linear function representing the good correspondence between predicted and measured data.

The models accuracy has been calculated by means of mean absolute percentage error (MAPE), mean squared error (MSE), root mean squared error (RMSE), relative root mean squared error (RRMSE), mean absolute error (MAE) and goodness of fit (R2). These indicators are provided by following equations [22]:

$$\mathrm{MSE} = \frac{1}{n}\sum_{i=1}^{n}\left(y_i - \widehat{y}_i\right)^2 \tag{4}$$

$$R^2 = \frac{\sum_{i=1}^{n}\left(\widehat{y}_i - \overline{y}\right)^2}{\sum_{i=1}^{n}\left(y_i - \overline{y}\right)^2} \tag{5}$$

$$\mathrm{RMSE} = \sqrt{\mathrm{MSE}} = \sqrt{\frac{1}{n}\sum_{i=1}^{n}\left(y_i - \widehat{y}_i\right)^2} \tag{6}$$

$$\mathrm{RRMSE} = \frac{\mathrm{RMSE}}{\overline{y}} \tag{7}$$

$$\mathrm{MAPE} = \frac{1}{n}\sum_{i=1}^{n}\frac{\left|\widehat{y}_i - y_i\right|}{y_i} \tag{8}$$

$$\mathrm{MAE} = \frac{1}{n}\sum_{i=1}^{n}\left|\widehat{y}_i - y_i\right| \tag{9}$$

where n is the dataset cardinality involved in this study, y_i represents the variable to calculate, $\overline{y}$ is the xmean value of y_i and $\widehat{y}_i$ is the value determined by model. MAPE estimates accuracy and RMSE is the standard deviation between predicted and actual values. It is parameter that allows the comparison of the forecasting error of different models referring to same variable. MAE measures how predictions and observed values are close, and R^2 calculates the ratio between the variation determined by regression model and the variation in sample data; it is an important parameter that determines the general regression model accuracy. Moreover, the accuracy of ANN and black-box models has been compared; the black-box model has been developed by authors and is valid in same ranges described by (2) and (3). It allows to calculate $P_{el,cell}$ by two relations valid in the ranges (2) and (3):

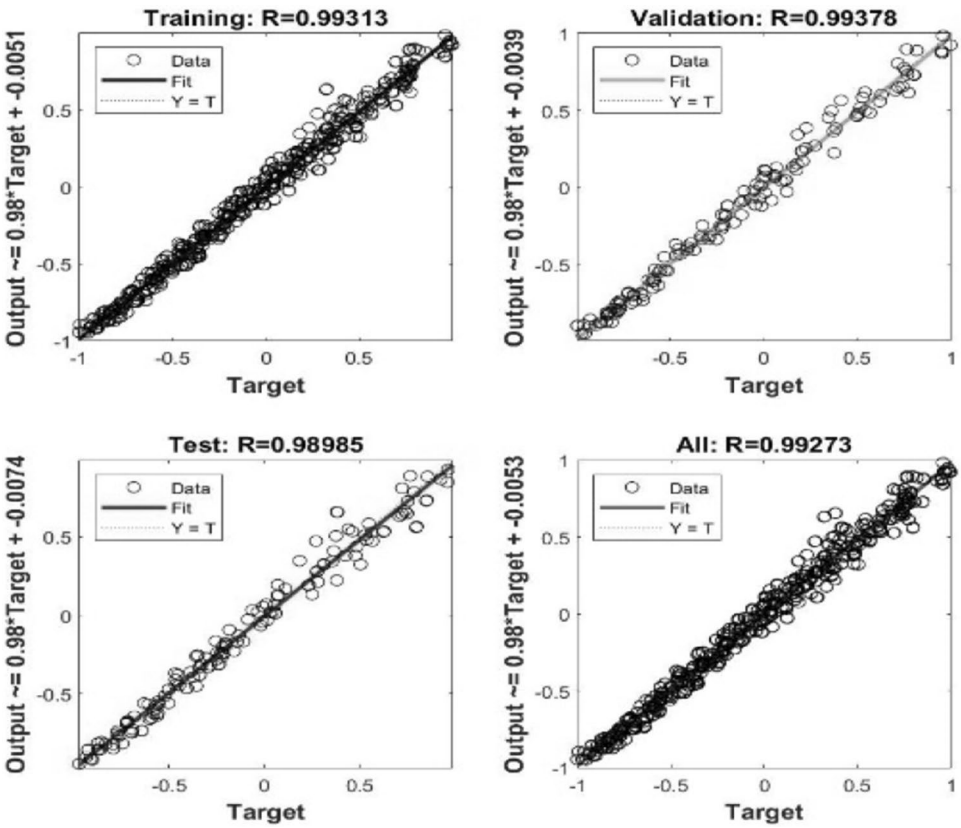

Fig. 4 Scatterplot of measured and predicted values for the phases of training, validation and test in case 1

$$P_{\text{el,cell}} = P_{\text{el,cell}}\left(I_{\text{cell}}, T_{\text{cell}}\right) = \begin{cases} 0.0080304\, x\, I_{\text{cell}} + 0.82818 \times T_{\text{cell}}^{-1} \\ 0.010790\, x\, I_{\text{cell}} - 1.4167 x 10^{-4} \times T_{\text{cell}}^{2} \end{cases} \quad (10)$$

The values of model parameters in (10) are $a_1 = 0.0080304 \pm 0.0001283$ and $a_2 = 0.82818 \pm 0.16443$. In (10), they are $b_1 = 0.010790 \pm 0.000109$ and $b_2 = (-1.4167 \pm 0.0734) \bullet 10^{-4}$.

The values of model parameters in (10) are $a_1 = 0.0080304 \pm 0.0001283$ and $a_2 = 0.82818 \pm 0.16443$. In (10), they are $b_1 = 0.010790 \pm 0.000109$ and $b_2 = (-1.4167 \pm 0.0734) \bullet 10^{-4}$. The values of these indicators both for ANN models and black-box model are reported in Table 3. The high value of R^2, very close to unity, highlights the good convergence achieved between measured and predicted values for both models. The very low values of the other error indicators show as well that each ANN model presents very good accuracy [22]. Moreover, the ANN models accuracy is higher with respect to the black-box models. In fact, by comparing them in terms of the most important indexes, it can be observed that ANN models show higher values of R^2 and lower values of the error indexes RRMSE and MAPE [22].

These models allow to calculate the electrical power supplied by single TJ cell. However, they can be also used to evaluate the energy production of CPV system. TJ cells in CPV system are generally organized in modules, whose electric power is given by [27]:

$$P_{\text{el, mod}} = P_{\text{el,cell}} \cdot f \cdot n_{c,\text{ mod}} \cdot \left(1 - p_{\text{par}}\right) \cdot \eta_{\text{mod}} \quad (11)$$

where $P_{\text{el, cell}}$ can be evaluated by ANN models developed in this study, $n_{\text{c,mod}}$ is the cells number per module, p_{par} is the loss factor representing parasitic current losses generated in the module, η_{mod} is the module efficiency that considers series coupling of cells along a line and the possibility of cell operating a less than nominal efficiency and with not ideal tracking system. Moreover, a factor f equal to 0.9 is considered. Hence, the electric power supplied by CPV system can be evaluated in this way:

$$P_{\text{el,CPV}} = P_{el,\text{ mod}} \cdot n_{\text{mod}} \cdot \eta_{\text{inv}} \quad (12)$$

where n_{mod} is the modules number that constitutes the plant and η_{inv} is inverter efficiency.

4 Results and discussion

The two ANN models introduced in this paper represent a good instrument for real energy performance evaluation of CPV system in wide range of working conditions. To

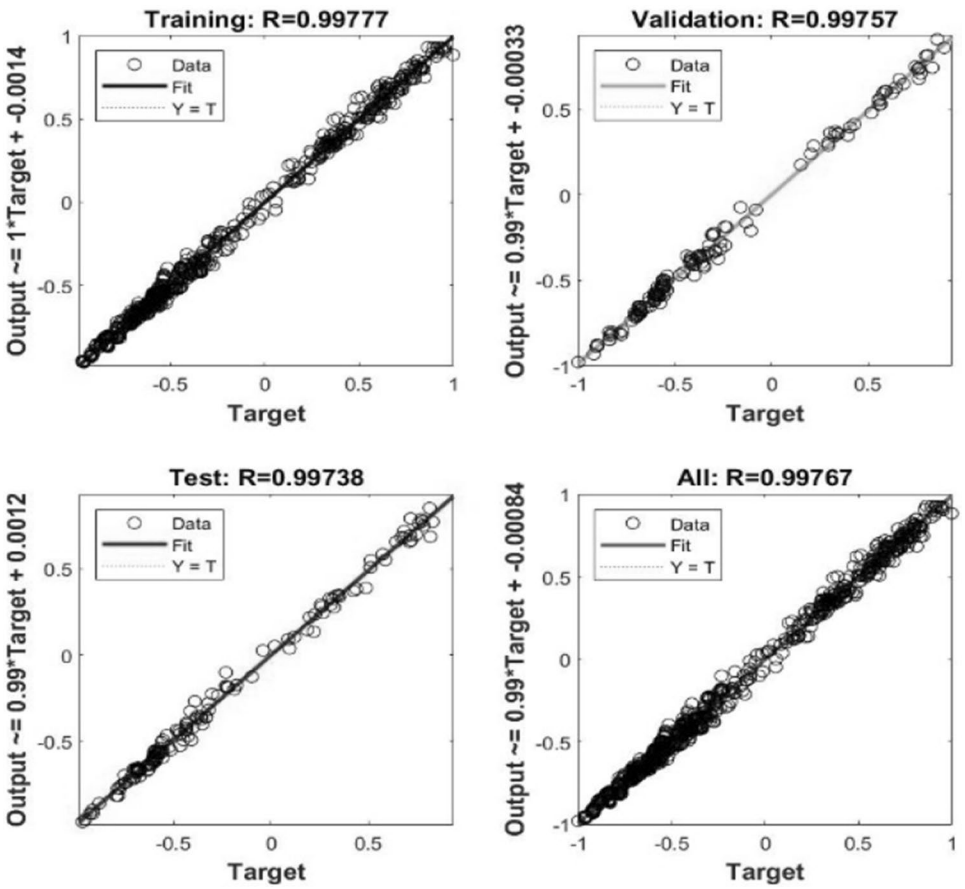

Fig. 5 Scatterplot of measured and predicted values for the phases of training, validation and test in case 2

Table 3 Values of different statistical indicators calculated for the two ANN models

Statistical indicator	Case 1		Case 2	
	ANN	Black-box	ANN	Black-box
MSE	$1.66 \bullet 10^{-4}$	//	$2.25 \bullet 10^{-3}$	//
R^2	0.993	0.977	0.998	0.979
RMSE	0.0129	//	0.0474	//
RRMSE	4.38%	7.97%	3.23%	10.15%
MAPE	3.49%	6.92%	2.66%	9.53%
MAE	0.00983	//	0.0359	//

demonstrate the accuracy of their results, in Fig. 6 the theoretical and experimental values of TJ cell electrical power are compared for both the ANN models referring to low-middle (a) and middle-high concentration (b) respectively. The experimental results shown in Fig. 6a have been collected during 25th June 2023 from 5:00 p.m. to 6:00 p.m and refer to C_{opt} equal to 80. Instead, the experimental results shown in Fig. 6b have been collected on 12th July 2023 from 10:00 a.m. to 11:00 a.m and refer to higher value of C_{opt} equal to 250.

It can be noted that both models show great accuracy since the measured and calculated electrical outputs show very similar trends both for low (a) and high (b) concentration. In particular, the uncertainty analysis shows that the average error is approximately 0.9% for low-medium concentration values, and about 1.3% for medium–high concentration values. A standard deviation value of 0.003 was also calculated for low-medium concentration values and 0.013 for medium–high concentration values. These results indicate a low dispersion of residuals compared to the mean, highlighting that the predicted values by the ANN model are very close to the theoretical values with minimal deviations. Hence, these models can be used to evaluate the energy performances of TJ solar cell in wide range of operation conditions, as described above. Considering the annual hourly distribution of DNI and T_{env} available in [28] and the rise of T_{cell} observed during the experimental activity, the ANN models developed allow to estimate the TJ cell electrical producibility during the year by varying concentration factor. In Fig. 7, the calculated TJ cell monthly electrical producibility for the city of Salerno (Italy) in correspondence with three values of concentration factor, is shown. It is clear that the electrical energy supplied is much variable

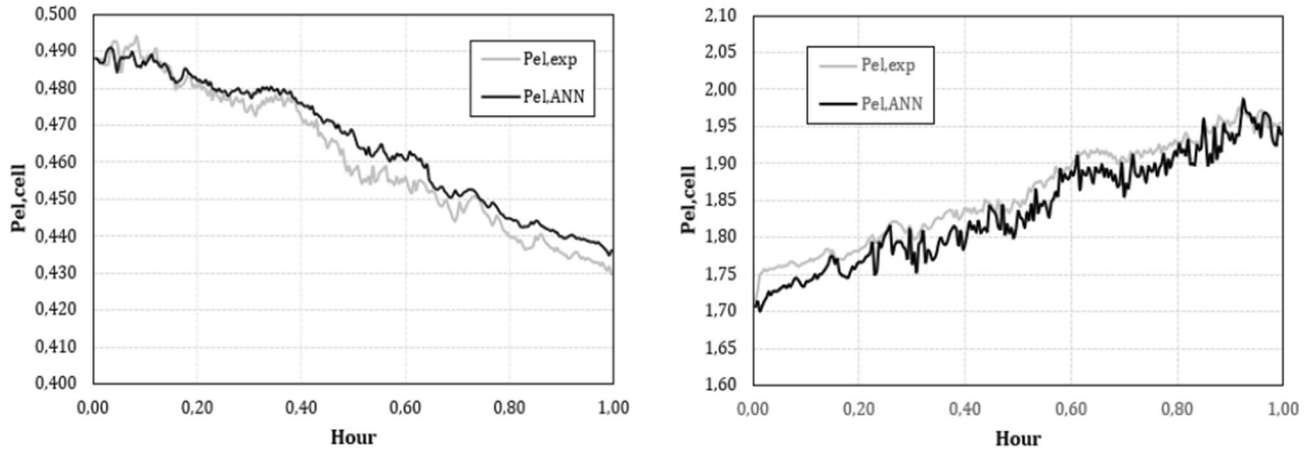

Fig. 6 Comparison between theoretical and experimental values of the TJ cell electrical power for low-middle (**a**) and middle-high concentration (**b**)

during the year and concentration factor is a key parameter for the increase of TJ cell producibility.

Starting from such results calculated for a single TJ cell, it is possible to size CPV systems to match their electrical producibility to energy demand of heterogeneous users. It is known that standard configurations do not exist in the CPV market. Hence, there are several possibilities and the most suitable for a certain application must be chosen according to the characteristics of the user to be powered.

In this study, a point-focus CPV system is dimensionated to match its electric power to energy demand of two different users, a residential building and an agricultural livestock farm located in Salerno (Italy). The users' electrical loads are shown in Fig. 8. The domestic user refers to house of 120 m^2 inhabited by 5 persons (Fig. 8a). The main activity of livestock farm is breeding of cattle and sheep for milk production. The facility comprises stable and farmhouse for the respective functions. In stable, electrical loads (Fig. 8b) are due to milking machines, refrigerators for milk preservation and lighting and machinery for barn cleaning. The electrical loads of farmhouse activity show more discontinuous trend (Fig. 8b).

A modular configuration of point-focus CPV system with 90 cells per module and concentration factor equal to 310, representing the maximum value experimentally achieved, is considered. The electric output of CPV system by varying its number of modules, has been determined using Eq. 12. Figure 9 illustrates the monthly difference between electrical energy generated by CPV system by varying its number of modules and electrical demand of each user.

The determination of the modules optimal number aims to maximize the investment profitability, as measured by NPV (Net Present Value). In Fig. 10, the NPV at 20th year, average useful life of CPV system, is reported as function of modules number for both users. The initial investment linked to CPV system cost, has been evaluated referring to cost

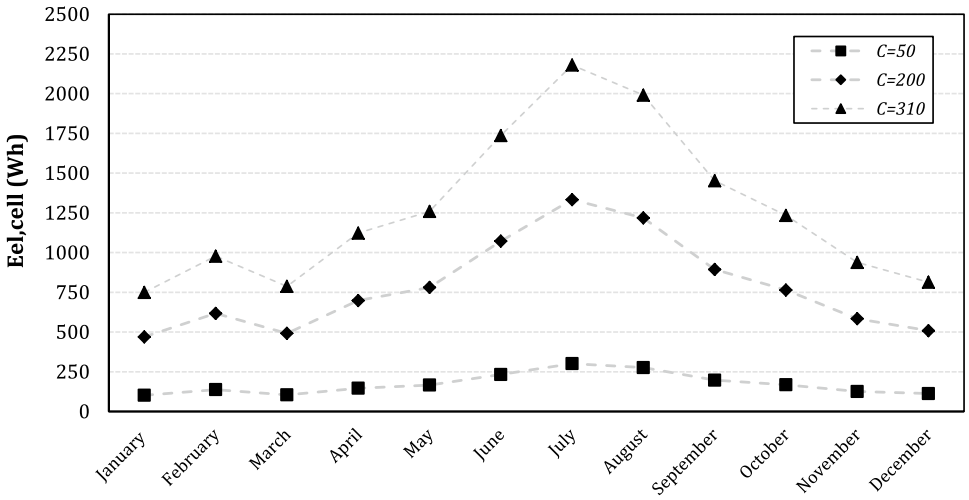

Fig. 7 TJ cell monthly electrical producibility for the city of Salerno (Italy) for three values of concentration factor

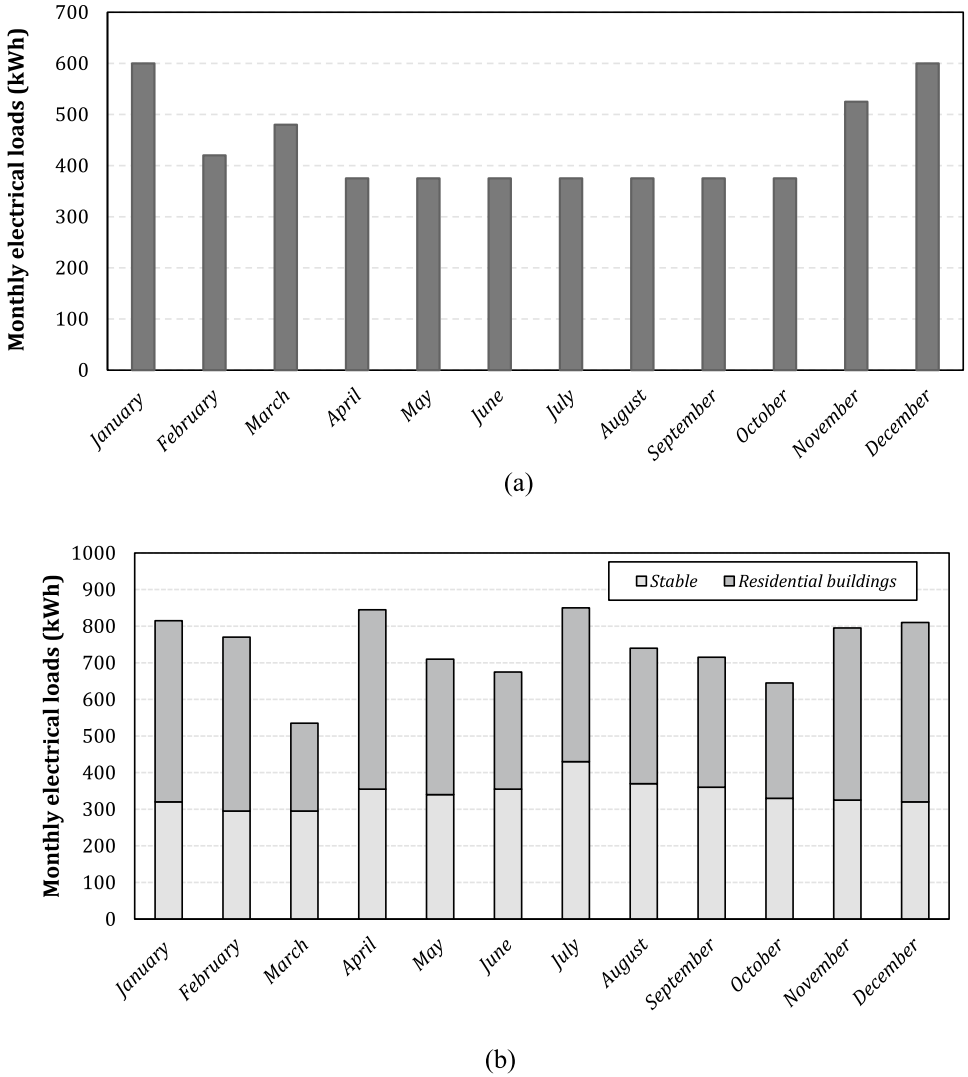

Fig. 8 Electric loads of domestic user (**a**) and livestock farm (**b**) to be powered

per unit of power equal to 2.94 €/W and discount rate equal to 0.015 [27]. The cash flow related to i-th year has been evaluated as sum of cost savings from purchasing required electricity and gains from selling surplus electrical energy. Specifically, unit purchase cost of electricity at 0.25 €/kWh and sale price to energy network of 0.06 €/kWh, have been considered.

As shown in Fig. 10, the NPV of investment rises when the modules number increases until its maximum value equal to 8.4 and 16.3 k€ for domestic user and livestock farm, respectively. If the modules number further increases, NPV decreases due to higher portion of CPV system electrical producibility sold to energy network at reduced price. Hence, optimal number of modules is equal to sixteen for CPV system used for domestic user and to thirty-six for livestock farm. By analyzing the NPV trend over time, it is also possible to evaluate the DPB (Discount Payback Period) of the investment (Fig. 11a, b), equal to 9.8 and 10.2 years for domestic user and livestock farm, respectively.

5 Conclusions

The purpose of paper has been the development of ANN model able to link electric power provided by CPV system with solar radiation and TJ cell temperature when C_{opt} changes. Two different ANN models referring to low and middle-high concentration values respectively have been developed. For both ANN models, the selected network has been an MLP, with two input neurons (corresponding to I_{cell} and T_{cell}, respectively), a hidden layer with ten neurons and an output neuron corresponding to $P_{el,\,cell}$. Each network adopts log-sigmoid function for transition from input to hidden layer and tan-sigmoid function for transition from hidden to output layer. The pre-processing of data was essential to enhance the efficiency of ANN training. The scatterplots of measured and predicted values for the three ANN modeling phases (training, validation, and test) and the values of several statistical indicators (MSE, MAPE, RMSE, RRMSE, MAE and R^2) have shown

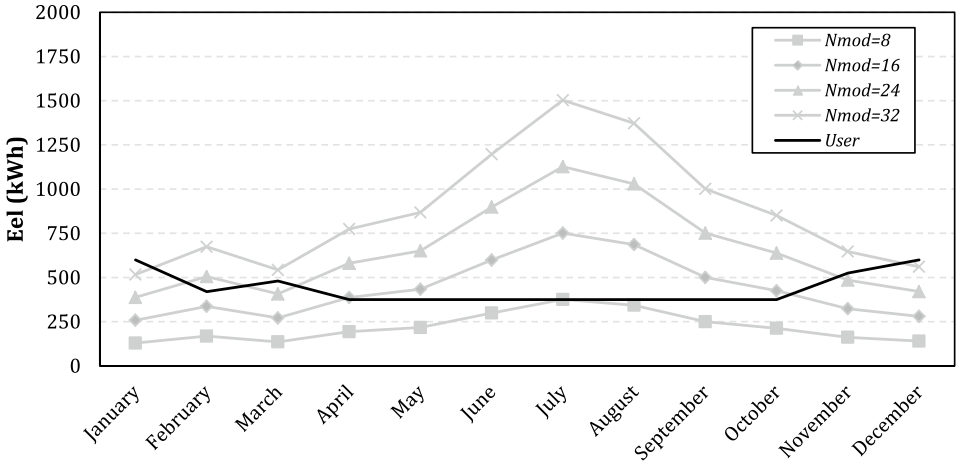

(a)

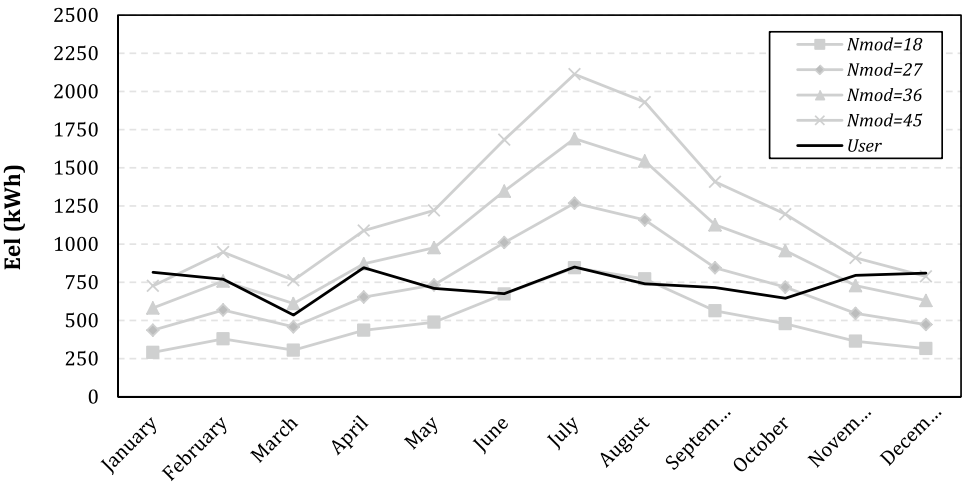

(b)

Fig. 9 Monthly difference between the CPV system electrical producibility by varying its number of modules and the electrical loads of domestic user (**a**) and livestock farm (**b**)

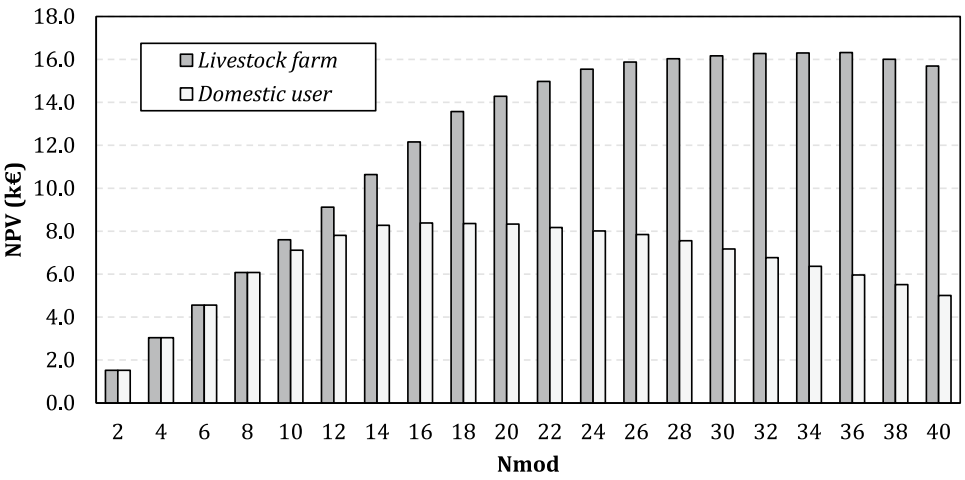

Fig. 10 NPV of the investment at the 20th year as a function of the number of modules for the two users analyzed

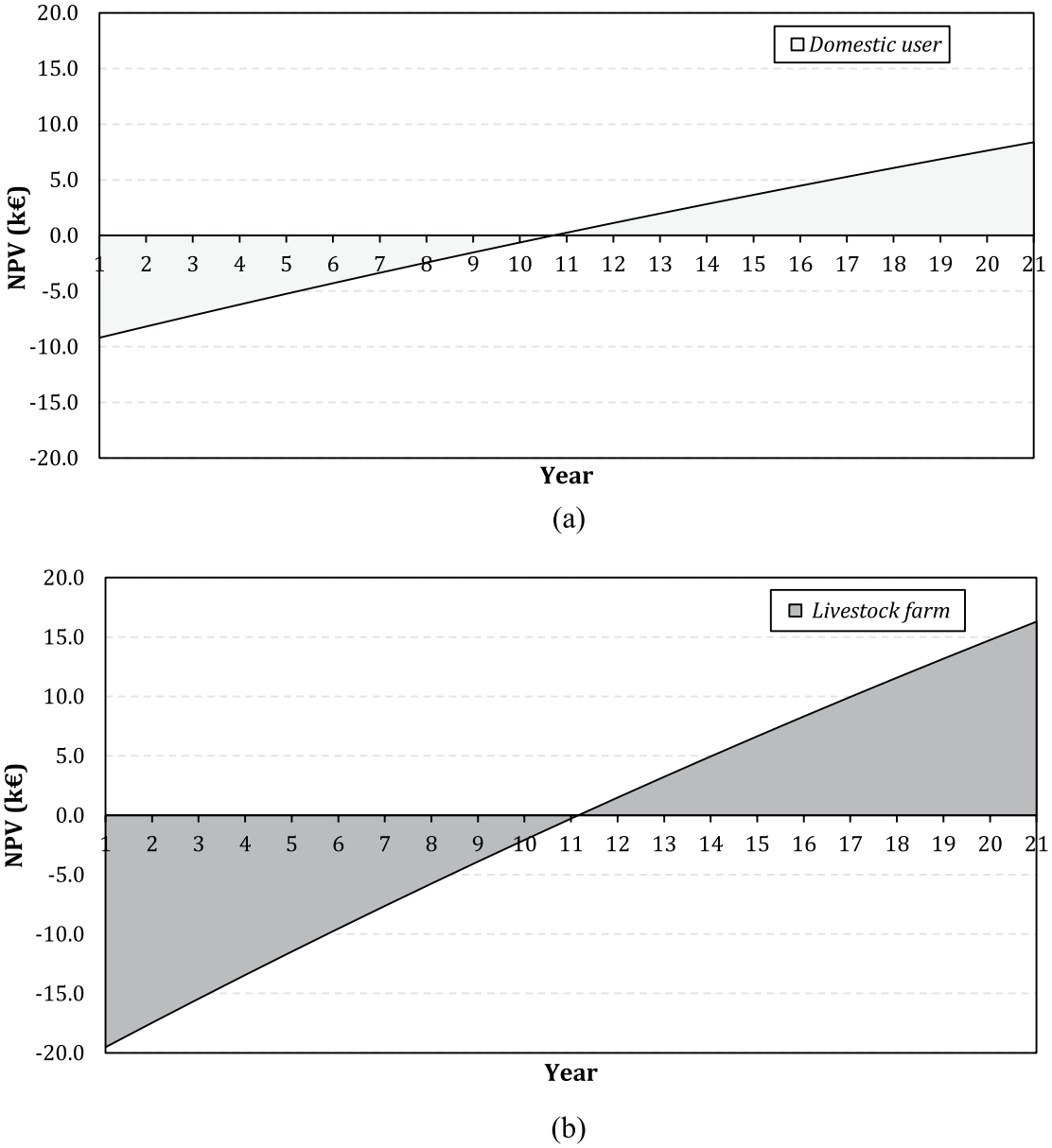

Fig. 11 NPV of the investment over the years for the two users analyzed

a very good accuracy, also confirmed by a comparison with another black-box model developed by authors.

The two ANN models have been employed to examine the monthly electrical producibility of TJ cell located in Salerno (Italy) by varying C_{opt}. Starting from these results, a point-focus CPV system has been sized to match its electric power to energy requirement of two different users: residential building and agricultural livestock farm.

A modular configuration of point-focus CPV system with 90 cells per module and concentration factor equal to 310 has been considered. After the investigation of the CPV system monthly producibility for each user, the number of modules has been established with the aim to optimize the NPV of the investment.

As for the residential user, a CPV system consisting of sixteen modules, with peak power of 3.1 kW and area of 130 m^2, allows the maximization of NPV value equal to 15.9 k€ with DPB of 9.8 years. As for the agricultural livestock, thirty-six modules, with peak power of 7.0 kW and area of 292 m^2, allow to maximize the NPV value equal to16.3 k€ with DPB of 10.2 years.

Referring to the future developments, there is considerable potential in adopting the ANN model developed in this

paper for other typologies of CPV point-focus systems working in same operation conditions.

Funding Open access funding provided by Università degli Studi di Salerno within the CRUI-CARE Agreement.

References

1. Wu Z, Xie G, Gao F, Chen W, Zheng Q, Liu Y (2024) Experimental study of a self-cooling concentrated photovoltaic (CPV) system using thermoelectric modules. Energy Convers Manage 299:117858
2. He X, Khan S, Ozturk I, Murshed M (2023) The role of renewable energy investment in tackling climate change concerns: environmental policies for achieving SDG-13. Sustain Dev 31:1888–1901
3. Renno C (2019) Thermal and electrical modelling of a CPV/T system varying its configuration. J Therm Sci 28:123–132
4. Maka AO, Alabid JM (2022) Solar energy technology and its role in sustainable development. Clean Energy 6(3):476–483
5. Wang G, Zhang Z, Chen Z (2023) Design and performance evaluation of a novel CPV-T system using a nanofluid spectrum filter with high solar concentration uniformity. Energy 267:126616
6. Renno C, Petito F (2018) Triple-junction cell temperature evaluation in a CPV system by means of a random-forest model. Energy Convers Manage 169:124–136
7. Martínez JF, Steiner M, Wiesenfarth M, Helmers H, Siefer G, Glunz SW, Dimroth F (2022) Global energy harvesting potential of CPV/PV hybrid technology. Arxiv Preprint. https://doi.org/10.48550/arXiv.2205.12858
8. Zubeer SA, Ali OM (2021) Performance analysis and electrical production of photovoltaic modules using active cooling system and reflectors. Ain Shams Eng j 12(2):2009–2016
9. Papis-Frączek K, Sornek K (2022) A review on heat extraction devices for CPVT systems with active liquid cooling. Energies 15(17):6123
10. Renno C (2020) Theoretical and experimental evaluation of the working fluid temperature levels in a CPV/T system. Energies 13:3077
11. Jacob J, Pandey AK, Abd Rahim N, Selvaraj J, Samykano M, Saidur R, Tyagi VV (2022) Concentrated photovoltaic thermal (CPVT) systems: recent advancements in clean energy applications, thermal management and storage. J Energy Storage 45:103369
12. Iqbal W, Ullah I, Shin S (2023) Optical developments in concentrating photovoltaic systems: a review. Sustainability 15(13):10554
13. Zayed ME, Zhad J, Li W, Sadek S, Elsheikh AH (2022) Applications of artificial neural networks in concentrating solar power systems. Artificial neural networks for renewable energy systems and real-world applications. Elsevier, Amsterdam, pp 45–67
14. Almonacid F, Rodrigo P, Fernández EF (2016) Determination of the current-voltage characteristics of concentrator systems by using different adapted conventional techniques. Energy 101:146–160
15. Alamin YI, Anaty MK, Álvarez HJD, Bouziane K, Pérez García M, Yaagoubi R, Aggour M (2020) Very short-term power forecasting of high concentrator photovoltaic power facility by implementing artificial neural network. Energies 13(13):3493
16. Kiran SR, Basha CH, Singh VP, Dhanamjayulu C, Prusty BR, Khan B (2022) Reduced simulative performance analysis of variable step size ANN based MPPT techniques for partially shaded solar PV systems. IEEE Access 10:48875–48889
17. Renno C, Petito F, Gatto A (2016) ANN model for predicting the direct normal irradiance and the global radiation for a solar application to a residential building. J Clean Prod 135:1298–1316
18. Renno C (2018) Experimental and theoretical analysis of a linear focus CPV/T system for cogeneration purposes. Energies 11:2960
19. Renno C (2022) Energy and economic comparison of three optical systems adopted in a point-focus CPV system. J Braz Soc Mech Sci Eng 44:1–11
20. Geetha A, Santhakumar J, Sundaram KM, Usha S, Thentral TT, Boopathi CS, Sathyamurthy R (2022) Prediction of hourly solar radiation in Tamil Nadu using ANN model with different learning algorithms. Energy Rep 8:664–671
21. Liang R, Le-Hung T, Nguyen-Thoi T (2022) Energy consumption prediction of air-conditioning systems in eco-buildings using hunger games search optimization-based artificial neural network model. J Build Eng 59:105087
22. Renno C, Petito F, Gatto A (2015) Artificial neural network models for predicting the solar radiation as input of a concentrating photovoltaic system. Energy Convers Manage 106:999–1012
23. Heng SY, Ridwan WM, Kumar P, Ahmed AN, Fai CM, Birima AH, El-Shafie A (2022) Artificial neural network model with different backpropagation algorithms and meteorological data for solar radiation prediction. Sci Rep 12(1):10457
24. Malik P, Gehlot A, Singh R, Gupta LR, Thakur AK (2022) A review on ANN based model for solar radiation and wind speed prediction with real-time data. Arch Comput Methods Eng 29:1–19
25. Ghimire S, Nguyen-Huy T, Prasad R, Deo RC, Casillas-Perez D, Salcedo-Sanz S, Bhandari B (2023) Hybrid perceptron model with multilayer convolutional neural network for solar radiation prediction. Cognit Comput 15(2):645–671
26. Matlab R2023b, The MathWorks
27. Renno C, D'Agostino D, Minichiello F, Petito F, Balen I (2019) Performance analysis of a CPV/T-DC integrated system adopted for the energy requirements of a supermarket. Appl Therm Eng 149:231–248
28. PVGIS, https://ec.europa.eu/jrc/en/pvgis